LETTERS

Adult satellite cells and embryonic muscle progenitors have distinct genetic requirements

Christoph Lepper[1,2], Simon J. Conway[3] & Chen-Ming Fan[1]

Myogenic potential, survival and expansion of mammalian muscle progenitors depend on the myogenic determinants *Pax3* and *Pax7* embryonically[1], and *Pax7* alone perinatally[2–5]. Several *in vitro* studies support the critical role of *Pax7* in these functions of adult muscle stem cells[5–8] (satellite cells), but a formal demonstration has been lacking *in vivo*. Here we show, through the application of inducible Cre/*loxP* lineage tracing[9] and conditional gene inactivation to the tibialis anterior muscle regeneration paradigm, that, unexpectedly, when *Pax7* is inactivated in adult mice, mutant satellite cells are not compromised in muscle regeneration, they can proliferate and reoccupy the sublaminal satellite niche, and they are able to support further regenerative processes. Dual adult inactivation of *Pax3* and *Pax7* also results in normal muscle regeneration. Multiple time points of gene inactivation reveal that *Pax7* is only required up to the juvenile period when progenitor cells make the transition into quiescence. Furthermore, we demonstrate a cell-intrinsic difference between neonatal progenitor and adult satellite cells in their *Pax7*-dependency. Our finding of an age-dependent change in the genetic requirement for muscle stem cells cautions against inferring adult stem-cell biology from embryonic studies, and has direct implications for the use of stem cells from hosts of different ages in transplantation-based therapy.

Skeletal muscle regeneration is of clinical importance to muscular dystrophies and sport injuries, and depends on a resident reservoir of muscle stem cells called satellite cells[10]. Satellite cells are set aside to become quiescent postnatally from a pool of highly proliferative muscle progenitors[1,11]. The survival and expansion of muscle progenitors rely on the transcription factor *Pax7*. As such, *Pax7* germline mutant mice which survive to adulthood have few or no myofibre-associated cells resembling satellite cells[2–5], and display severely compromised muscle regeneration[3,4]. Although it remains controversial whether *Pax7* mutant myofibre-associated cells are myogenic *in vivo*[3,4], *in vitro* studies corroborate the role of *Pax7* in myoblast survival, proliferation and the establishment of myogenic potential[5,7,8]. Together with persistent *Pax7* expression in adult quiescent satellite cells[2,12], these data have raised the expectation that adult muscle stem-cell self-renewal and injury-induced muscle regeneration depend on *Pax7*. Thus, we examined these highly anticipated roles of *Pax7 in vivo*.

To determine *Pax7* function in adult satellite cells, we bypassed its earlier requirement via temporal gene inactivation in the adult. Previous analyses of *Pax7* mutants without lineage tracing have led to conflicting conclusions[3,4]. Therefore, we labelled conditionally inactivated *Pax7* cells and tracked their fate. Two new *Pax7* alleles were generated: $Pax7^{f}$, a conditional allele, which after Cre-mediated recombination becomes the null allele $Pax7^{\Delta}$ (Supplementary Fig. 1); and $Pax7^{CE}$ which expresses a tamoxifen-inducible Cre recombinase–oestrogen receptor fusion protein, $CreER^{T2}$ (ref. 13), in place of *Pax7*, and is therefore also null for *Pax7* (Supplementary Fig. 2). We assayed for inducible Cre activity by crossing $Pax7^{CE}$ mice to *Rosa26* reporter (*R26R*) mice[14], which express *lacZ* after Cre-mediated recombination (Supplementary Fig. 3). Tamoxifen-dependent $CreER^{T2}$ activity was confirmed by β-gal activity (X-galactosidase reaction). Efficacy and specificity of tamoxifen-induced satellite cell labelling was confirmed by 99.8% co-localization of β-gal and Pax7 in tibialis anterior muscles (Supplementary Fig. 3).

The $Pax7^{CE}$ and $Pax7^{f}$ alleles were combined ($Pax7^{CE/f};R26R^{+/-}$) for conditional inactivation of *Pax7* between postnatal days 60–90 (P60–90) by tamoxifen. After five daily tamoxifen injections (see Methods; Fig. 1a, b), no wild-type *Pax7* transcript, no Pax7 protein and no $Pax7^{+}$ cells were detected in tibialis anterior muscles (Supplementary Fig. 4). Conditional *Pax7* inactivation in adult satellite cells did not lead to loss of $\beta\text{-gal}^{+}$ cells (Supplementary Fig. 5), indicating that *Pax7* is not required for their survival. Conditional mutant cells maintain satellite cell characteristics as shown by M-cadherin (M-Cad), CD34, and integrin β1 and α7 expression[15,16] (Supplementary Fig. 6).

To determine if *Pax7* conditional mutant cells can support injury-induced myogenesis, we used cardiotoxin to induce injury. In *Pax7* heterozygotes ($Pax7^{+/CE};R26R^{+/-}$), all regenerating fibres at days 5 and 10 after injury are $\beta\text{-gal}^{+}$ (Fig. 1c, d and Supplementary Fig. 7). This result provides unequivocal evidence that *Pax7* descendants are a major source of regenerating myofibres, extending data[15] that single $Pax7^{+}$ cells can form myofibres after transplantation into tibialis anterior muscles. Contrary to expectation, regenerative myogenesis from *Pax7* descendants was not impaired in conditional *Pax7* mutants ($Pax7^{CE/f};R26R^{+/-}$) as assessed by X-galactosidase reactions (Fig. 1e, f), regenerated fibre size (Fig. 1g, h) and number (Supplementary Fig. 7). No reappearance of wild-type *Pax7* mRNA or protein was detected in injured muscles 10 days after injury (Fig. 1i, j). Thus, *Pax7* is not required for injury-induced myogenesis in adulthood.

These results contrast with *Pax7* germline mutants where only a minimal number of small regenerative myofibres are found after injury (refs 3, 4 and Supplementary Fig. 1). These sparse regenerated fibres were proposed to be derived from alternative source(s), that is, non-*Pax7* lineage[4]. To test this, we assayed for injury-induced myogenesis in surviving $Pax7^{CE/CE};R26R^{+/-}$ adults using the experimental paradigm described above. Surprisingly, the rare regenerative myofibres (Fig. 1k, l) were all of *Pax7* descent. This result indicates that *Pax7* germline mutant cells surviving to adulthood do have myogenic potential and argues against alternative non-*Pax7* sources.

Isolated surviving cells associated with myofibres in adult *Pax7* germline nulls lack typical satellite cell characteristics[4]. Therefore, we examined whether conditional *Pax7* mutant cells also lose satellite cell characteristics after supporting one round of regeneration. For this,

[1]Department of Embryology, Carnegie Institution, 3520 San Martin Drive, Baltimore, Maryland 21218, USA. [2]Department of Biology, Johns Hopkins University, 3400 North Charles Street, Baltimore, Maryland 21218, USA. [3]Riley Heart Research Center, Herman B Wells Center for Pediatric Research, Indiana University School of Medicine, Indianapolis, Indiana 46202, USA.

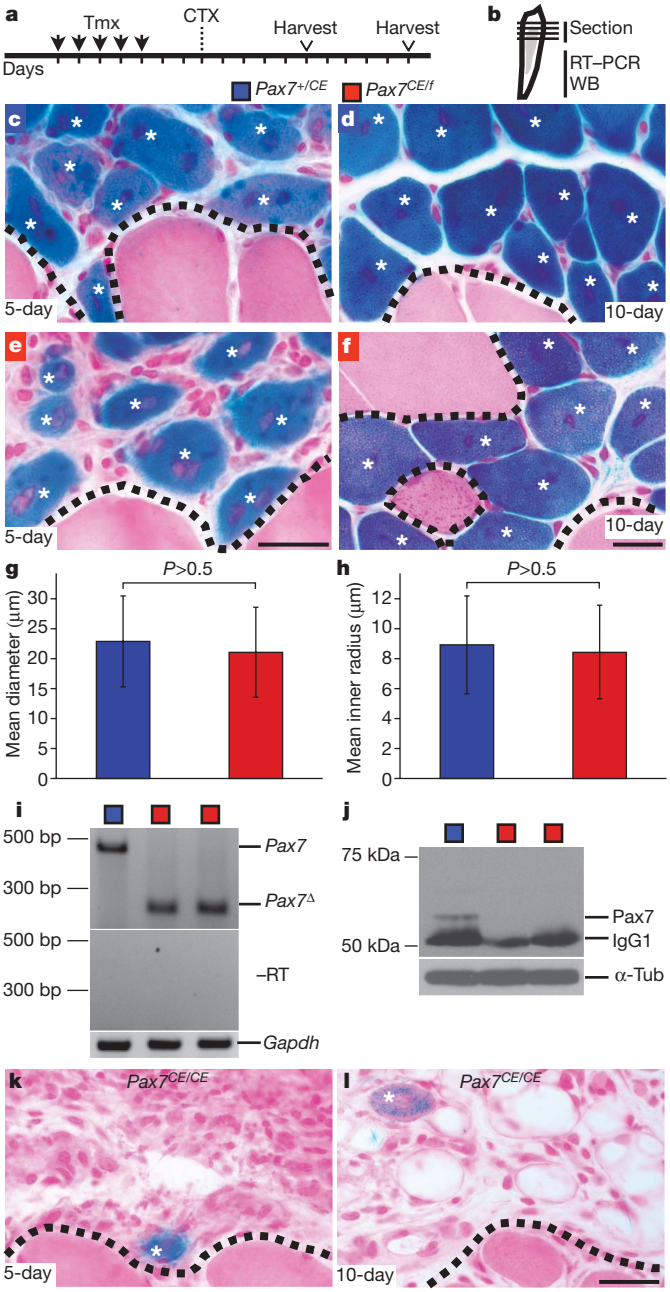

Figure 1 | Adult-specific *Pax7* mutant cells regenerate muscle efficiently. **a**, Tamoxifen (Tmx) and cardiotoxin (CTX) regimen and regeneration assay scheme. Vertical lines indicate daily intervals. **b**, Tibialis anterior muscle diagram with injury in grey. Horizontal lines indicate cross-sections; WB, western blot. **c**–**f**, β-gal (by X-galactosidase reaction) and nuclear fast red (NFR) stained $Pax7^{+/CE}$ (**c**, **d**) and $Pax7^{CE/f}$ (**e**, **f**) muscles at 5 (**c**, **e**) and 10 (**d**, **f**) days after injury. Asterisks indicate regenerating fibres with central nuclei; dashed lines indicate boundary of injury. **g**, **h**, Mean diameter (**g**) and mean inner radius (**h**) of 10-day regenerated β-gal$^+$ fibres; 300 fibres per animal ($n = 3$ per genotype); error bars indicate s.d.; *P*, two-tailed Student's *t*-test. **i**, **j**, RT–PCR (**i**) and western blot (**j**) of examples of $Pax7^{+/CE}$ and $Pax7^{CE/f}$ (two shown) muscles; wild-type *Pax7* and recombined ($Pax7^{\Delta}$) transcripts are indicated; −RT control, *Gapdh* control, endogenous IgG1 and α-tubulin (α-Tub, loading control) are indicated. **k**, **l**, β-gal and NFR stained $Pax7^{CE/CE}$ muscles at 5 (**k**) and 10 (**l**) days after injury; regimen in **a**. All animals were $R26R^{+/-}$. Scale bars: 25 µm for **c**, **e** (shown in **e**), **d**, **f** (shown in **f**) and **k**, **l** (shown in **l**).

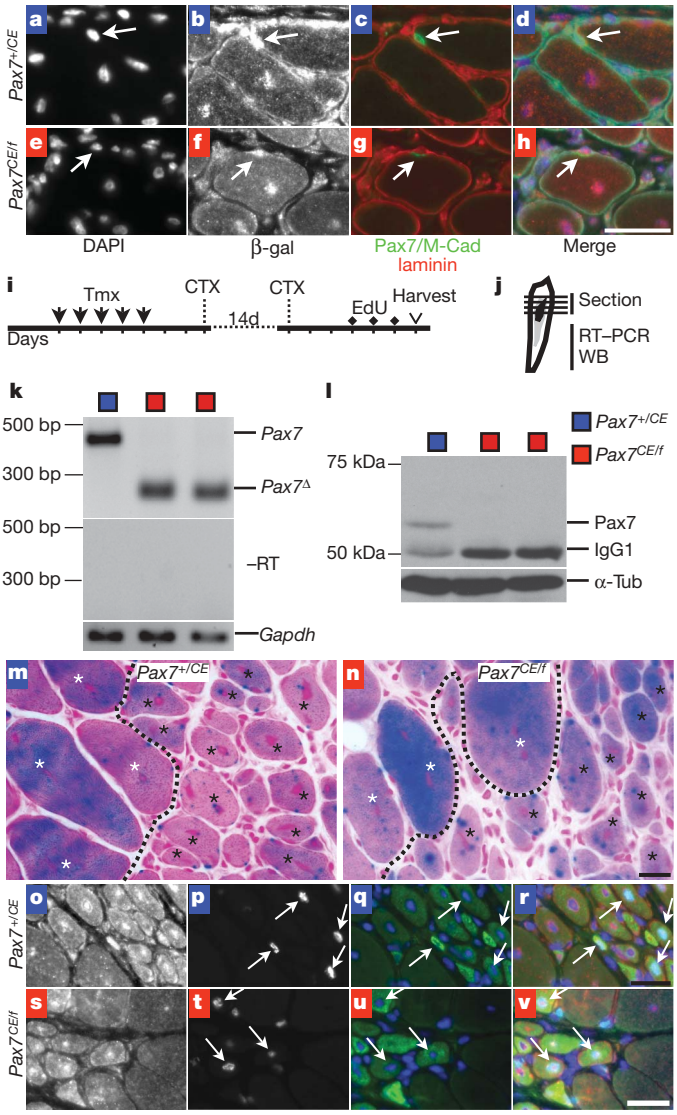

Figure 2 | Adult-specific *Pax7* mutant cells are functional satellite cells. **a**–**h**, Fluorescent microscopy of $Pax7^{+/CE}$ (**a**–**d**) and $Pax7^{CE/f}$ (**e**–**h**) 10-day regenerates. **a**, **e**, DAPI. **b**, **f**, β-gal. **c**, **g**, Laminin (red), Pax7 and M-Cad (both in green: Pax7, nuclear; M-Cad, satellite–muscle junction). **d** and **h** are merged from **a**–**c** and **e**–**g**, respectively; β-gal pseudo-coloured in red, DAPI in blue, laminin in cyan, Pax7 and M-Cad in green; white arrows indicate satellite cells. **i**, Double injury regeneration assay scheme with EdU injections; labelling as in Fig. 1a with 14 days (14d) between two injuries. **j**, Tibialis anterior muscle diagram with first injury in grey and second injury in black. **k**, **l**, RT–PCR (**k**) and western blot (**l**) of tibialis anterior muscles after second injury; labelling as in Fig. 1i, j. **m**, **n**, β-gal and NFR stained $Pax7^{+/CE}$ (**m**) and $Pax7^{CE/f}$ (**n**) regenerates at day 6 after second injury; dashed lines indicate boundaries between first and second regenerations based on differences in fibre size; white and black asterisks indicate old and new regenerated fibres, respectively. All fibres are β-gal$^+$ compared to interstitial cells, but with varying staining signals. **o**–**v**, Fluorescent microscopy of $Pax7^{+/CE}$ (**o**–**r**) and $Pax7^{CE/f}$ (**s**–**v**) regenerates. **o**, **s**, β-gal. **p**, **t**, EdU. **q**, **u**, RNMy2/9D2 (green) and DAPI (blue). **r** and **v** are merged from **o**–**q** and **s**–**u**, respectively; β-gal in red and other colours are the same as panels to the left; EdU$^+$ nuclei are indicated by white arrows. Scale bars: 25 µm for **a**–**h** (shown in **h**), **m**, **n** (shown in **n**), **o**–**r** (shown in **r**) and **s**–**v** (shown in **v**).

β-gal-marked cells were assessed for satellite niche occupancy using anti-M-Cad (for satellite/muscle junction) and anti-laminin (for basal lamina). We found β-gal$^+$M-Cad$^+$Pax7$^+$ satellite cells in the sublaminal space in control regenerated tissue (Fig. 2a–d and Supplementary Fig. 8). Surprisingly, sublaminal β-gal$^+$M-Cad$^+$Pax7$^-$ cells were also found in *Pax7* conditional mutants (Fig. 2e–h). When we used 5-ethynyl-2′-deoxyuridine (EdU) to monitor cells that had undergone proliferation, we found EdU$^+$ myonuclei and EdU-retaining sublaminal β-gal$^+$M-Cad$^+$Pax7$^-$ cells in conditional mutants (Supplementary Fig. 8). We did not detect any Pax7$^+$ or β-gal$^-$M-Cad$^+$ sublaminal cells

in *Pax7*-inactivated regenerates, arguing against compensation by other lineages with or without *de novo Pax7* activation. These data indicate that adult-specific *Pax7* mutant descendants not only form muscle fibres but also proliferate and occupy the satellite niche.

To determine whether the β-gal$^+$M-Cad$^+$Pax7$^-$ sublaminal cells in conditional mutant regenerates still have myogenic potential, we induced a second round of injury (Fig. 2i, j). Twenty-eight days after the first tamoxifen injection, neither wild-type *Pax7* mRNA nor protein was detected in doubly injured conditional *Pax7* mutants (Fig. 2k, l). We found that small and large β-gal$^+$ fibres were comparable between controls (Fig. 2m) and conditional mutants (Fig. 2n) 6 days after the second injury. To identify second-round regenerated myofibres, we used the RNMy2/9D2 antibody, which labels new fibres only up to 6 days after injury[17]. Within the β-gal$^+$ regenerated area, small fibres were RNMy2/9D2$^+$ in control animals (Fig. 2o, q, r) and conditional mutants (Fig. 2s, u, v). To assess whether *Pax7* descendants had proliferated before forming new fibres, EdU was administered after the second injury. Indeed, we found EdU$^+$ nuclei in RNMy2/9D2$^+$ fibres of control animals (Fig. 2p, r) and conditional mutants (Fig. 2t, v). Although we cannot formally exclude contribution from *Pax7*-independent lineages, our data suggest that adult-inactivated *Pax7* mutant cells can repeatedly contribute to muscle regeneration.

The normal regenerative capacity of conditional *Pax7* mutants sharply contrasts with the severe germline *Pax7* mutant defects (refs 3, 4 and here), and indicates the possibility of adult-specific compensation by another *Pax* family member. *Pax3* is a likely candidate as *Pax3* and *Pax7* compensate for each other in embryonic myogenesis[1]. We detected *Pax3* transcripts in adult tibialis anterior muscles (Fig. 3a) but not Pax3 protein (not shown). To determine whether *Pax3* can compensate for *Pax7* in adult myogenesis, we conditionally inactivated both genes in adulthood. We used the *cre/Esr1* allele[18], which directs ubiquitous tamoxifen-inducible Cre activity, to conditionally recombine a *Pax3* floxed allele, *Pax3^f* (ref. 19). After the tamoxifen regimen in Fig. 1a, both *Pax3^f* and *Pax7^f* were recombined (Fig. 3a, b). Surprisingly, muscle regeneration was not impaired in *Pax3;Pax7* doubly inactivated tibialis anterior muscles as assessed by histology (Fig. 3d, compared to control in panel c) and regenerated fibre size (Fig. 3i, j). Furthermore, we found sublaminal M-Cad$^+$Pax7$^-$ cells within the regenerate (Fig. 3g, h; compare to the control M-Cad$^+$Pax7$^+$ cells, Fig. 3e, f). Thus, contrary to their essential roles for embryonic myogenesis, neither *Pax3* nor *Pax7* is required during adult tibialis anterior muscle regeneration.

We next determined if and when myogenic progenitors become independent of *Pax7 in vivo*. To test this, we conditionally inactivated *Pax7* at different postnatal time points. Animals were then injured and regeneration was assessed 10 days later. When *Pax7* was inactivated between P7–11, regeneration was severely compromised (Fig. 4b). However, when inactivation was carried out at P14–18 and P21–25 (Fig. 4c, d), regenerative capacity gradually increased to levels similar to control mice (Fig. 4a). Notably, regenerated fibres were *Pax7* descendants (β-gal$^+$). Thus, *Pax7* function is critical before P21. To elucidate muscle progenitor behaviour at this postnatal period, we performed lineage tracing and found that myofibre fusion from *Pax7* descendants sharply declines by P21 (Supplementary Fig. 9), suggesting a transition to quiescent satellite cells. Intriguingly, myonuclei positioning in regenerated fibres also differs between P21 and adult animals, suggesting a coordinated transition of muscle biology around P21 (ref. 20). By contrast, myofibre incorporation by *Pax7*-mutant descendants occurs for a prolonged period (beyond P31, Supplementary Fig. 9), indicating that mutant cells have a greater propensity to differentiate. We therefore propose that in addition to survival and proliferation[3,5], *Pax7* also directs myogenic progenitors to withdraw from myogenic differentiation and transition into quiescent satellite cells, thereby acquiring maximum regenerative capacity.

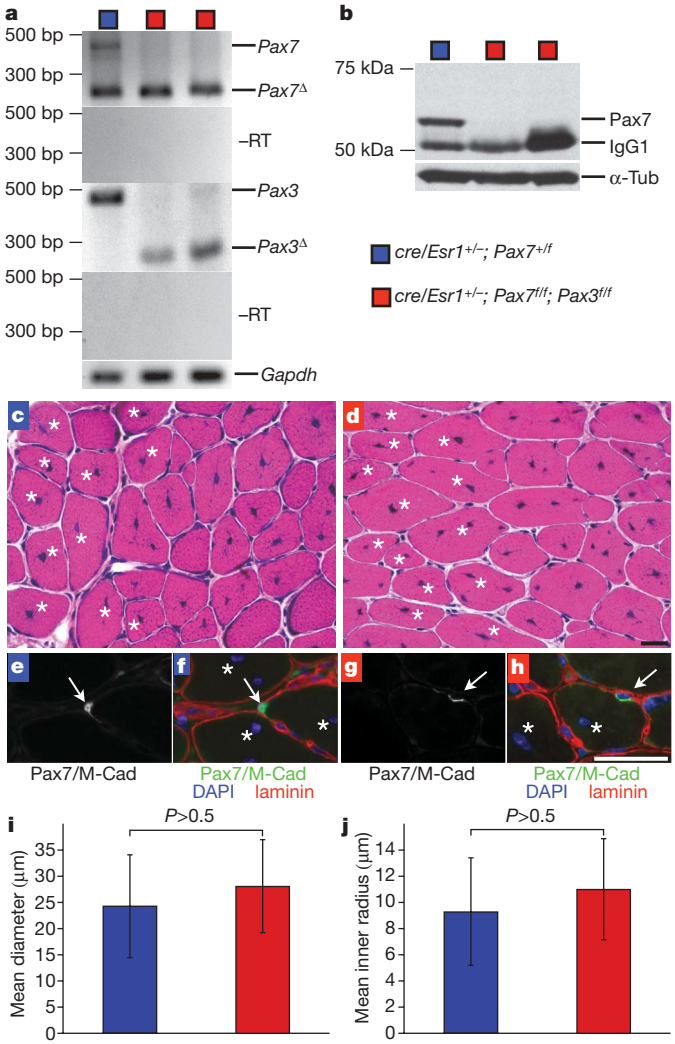

Figure 3 | *Pax3* and *Pax7* are dispensable for adult muscle regeneration. **a**, **b**, RT–PCR (**a**) and western blot (**b**) of indicated genotypes from the regeneration assay scheme in Fig. 1a. Labelling is the same as Fig. 1i, j, with additions of *Pax3* wild type and recombined (*Pax3$^\Delta$*) transcripts. **c**–**h**, *cre/Esr1$^{+/-}$;Pax7$^{+/f}$* (**c**, **e**, **f**) and *cre/Esr1$^{+/-}$;Pax7$^{f/f}$;Pax3$^{f/f}$* (**d**, **g**, **h**) day-10 regenerated muscles. **c**, **d**, Haematoxylin and eosin stain. **e**, **g**, Fluorescent microscopy of Pax7 and M-Cad together (arrowheads, M-Cad$^+$ cells). **f** and **h** are coloured composites with co-stained laminin (red), DAPI (blue) and Pax7/M-Cad (green) of **e** and **g**, respectively; asterisks indicate central nuclei whereas arrows indicate satellite cells. **i**, **j**, Mean diameter (**i**) and mean inner radius (**j**) of regenerated fibres; 300 fibres per animal ($n = 3$ per genotype). Error bars indicate s.d.; *P*, two-tailed Student's *t*-test. Scale bars: 25 μm for **c**, **d** (shown in **d**) and **e**–**h** (shown in **h**).

To determine whether this temporal difference is a cell-intrinsic or environmental effect, we cultured myoblasts isolated from *Pax7$^{+/CE}$;R26R$^{+/-}$* and *Pax7$^{CE/f}$;R26R$^{+/-}$* tibialis anterior muscles at P0 (before quiescence) and P60 (after becoming quiescent), and assayed their properties after tamoxifen treatment. Compared to controls, conditional *Pax7*-inactivated P0 myoblasts (β-gal$^+$) were defective in expansion and myogenic potential (Fig. 4e–g). At passage 1, residual conditional mutant cells still expressed desmin (Fig. 4g, k), displayed fibroblastic morphology at a high frequency (Fig. 4g), and some were positive for the fibroblastic marker ER-TR7 (Fig. 4g, l); however, many cells are of unknown fate(s) as they do not express either marker. This is in contrast to controls (Fig. 4g), reminiscent of aged *Pax7*-descendant cells after losing *Pax7* expression *in vitro*[21]. After passage 2, mutant cells were no longer myogenic (not shown) and most β-gal$^+$ cells were fibroblastic. Thus, inactivation of *Pax7* in neonatal myoblasts *in vitro* decreases their expansive and myogenic capacity. In contrast, control and conditionally inactivated *Pax7*-descendant adult

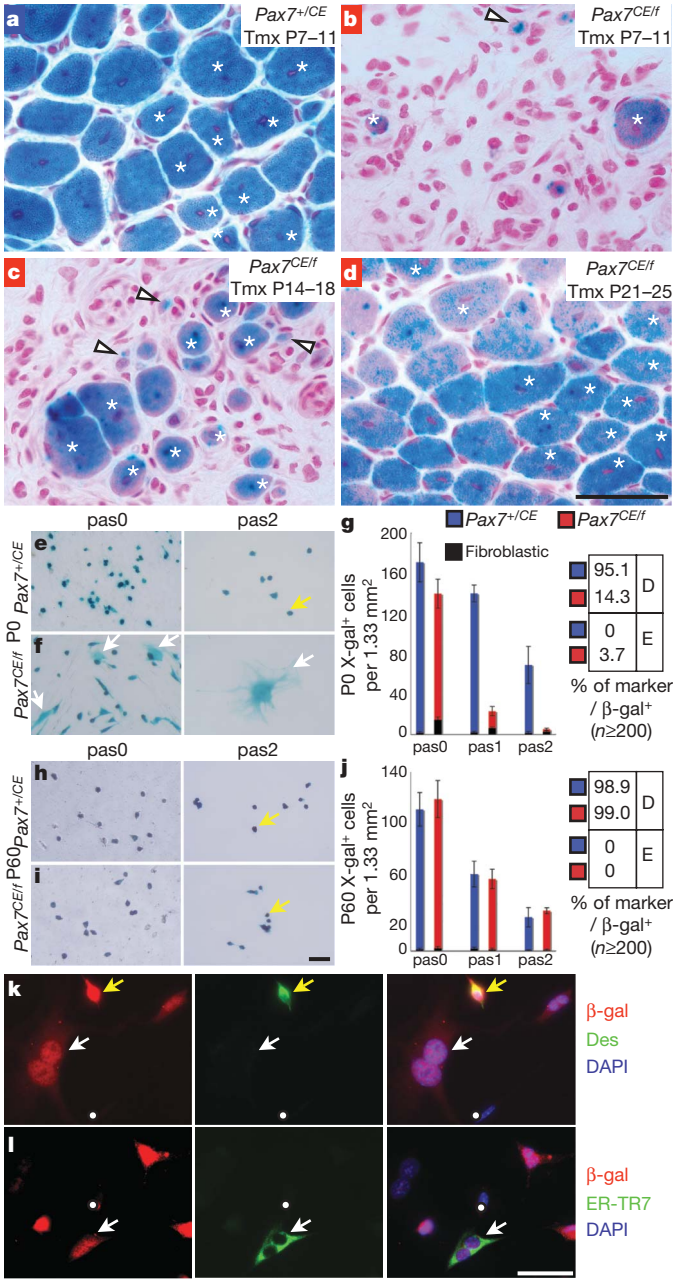

Figure 4 | Age-dependent intrinsic change of *Pax7* requirement. **a–d**, Regeneration assessed at day 10 by β-gal and NFR staining. **a**, Control ($Pax7^{+/CE}$) regenerates of P7–11 tamoxifen-treated sample; essentially the same for other time points (not shown). **b–d**, Conditional inactivation of *Pax7* ($Pax7^{CE/f}$) by tamoxifen at P7–11 (**b**), P14–18 (**c**) and P21–25 (**d**), followed by injury at P21 for **b**, **c** and P26 for **d**. RT–PCR confirmed complete *Pax7* inactivation (not shown). Asterisks indicate new fibres; arrowheads indicate β-gal$^+$ cells; $n = 3$ each; all are $R26R^{+/-}$. **e–j**, P0 (**e–g**) and adult (P60, **h–j**) tamoxifen-treated (0.4 μM) and β-gal-stained $Pax7^{+/CE}$;$R26R^{+/-}$ (**e**, **h**) and $Pax7^{CE/f}$;$R26R^{+/-}$ (**f**, **i**) myoblasts at passages 0 (pas0, left panels of **e**, **f**, **h**, **i**) and 2 (pas2, right panels of **e**, **f**, **h**, **i**). Yellow arrows indicate round/short-spindled myoblasts; white arrows indicate fibroblastic cells. **g**, **j**, Left: average cell numbers (≥9 fields) at each passage (*x* axis); $n = 3$ per genotype per stage; error bars indicate s.d. Right: percentages of desmin$^+$ (D) and ER-TR7$^+$ (E) of β-gal$^+$ cells at passage 1 ($n \geq 200$ each). **k**, **l**, Fluorescent microscopy of tamoxifen-treated P0 $Pax7^{CE/f}$;$R26R^{+/-}$ myoblasts at passage 1. β-gal (left panels of **k**, **l**), desmin (centre panel of **k**), ER-TR7 (centre panel of **l**) and merged with DAPI (right panel of **k** is a merge of left and centre panels; right panel of **l** is a merge of left and centre panels); yellow arrows indicate desmin$^+$ cells; white arrows indicate ER-TR7$^+$ or fibroblastic cells; white dots indicate negative cells for reference. Note β-gal staining and immunofluorescence in nuclei. Scale bars: 50 μm for **a–d** (shown in **d**), **e**, **f**, **h**, **i** (shown in **i**) and **k**, **l** (shown in **l**).

myoblasts had comparable expansive and myogenic potentials (Fig. 4h–j) as well as myogenic differentiation capacity (Supplementary Fig. 10). No β-gal$^+$ER-TR7$^+$ cells were found despite the presence of rare fibroblastic cells (Fig. 4j). Tamoxifen-treated *cre/Esr1*$^{+/-}$;*Pax7*$^{f/f}$;*Pax3*$^{f/f}$ adult myoblasts also had comparable proliferative and myogenic properties as mock-treated controls (Supplementary Fig. 11). Together, these data support a cell-autonomous change within satellite cells compared to their progenitor state.

We have defined a critical period of *Pax7* dependency in the transition from muscle progenitor to adult stem-cell state, which ensures that muscles achieve regenerative capacity. Given the essential roles for *Pax3* and *Pax7* in embryonic and for *Pax7* alone in perinatal myogenic progenitors, it was entirely unexpected that adult satellite cells require neither *Pax7* nor *Pax3* for muscle regeneration. We imagine that postnatal changes of muscle organization, mechanics and physiology demand stem cells to alter their transcriptional program as a means to adapt to these challenges. Changes in genetic requirement for muscle stem cells from embryonic to juvenile to adult stages elucidate the inadequacy of applying knowledge gained from developmental studies to adult stem-cell biology. Our discovery should encourage future investigations into how widespread genetic transitions may occur in different adult stem-cell types. Age-dependent differences in stem-cell properties should also urge careful consideration of the age of stem cells used in transplantation-based regenerative medicine.

METHODS SUMMARY

Animals. *Pax7*^{f} and *Pax7*^{CE} alleles are described in Supplementary Figs 1 and 2. The *Pax3*^{f} allele was described previously[19]. *R26R* (ref. 14) and *cre/Esr1* (ref. 18) mice were from the Jackson Laboratory. Tamoxifen (Sigma) was administered intraperitoneally (animals >2 weeks) or subcutaneously (<2 weeks) at 3 mg per 40 g body weight per injection. Cardiotoxin (10 μM, Sigma) was injected into tibialis anterior muscles (after anaesthesia) at 100 μl (animals >2 months) and 50 μl (<2 months). EdU (Invitrogen) was injected at 0.1 mg per 20 g bodyweight per injection. All procedures were approved by IACUC.

PCR genotyping, RT–PCR and western blot. Primers used for genotyping and RT–PCR are in Supplementary Tables 1 and 2. Antibodies used for western blots are in Supplementary Tables 3 and 4, and ECL (Amersham) was used for detection.

X-galactosidase reactions, immunofluorescence and histology. Tibialis anterior muscles were fresh frozen in isopentane/liquid nitrogen and cryo-sectioned at 10 μm. X-galactosidase (Qiagen) reactions followed standard procedure[22]; counterstained by NFR (Lab Vision). Immunofluorescence was performed using antibodies in Supplementary Tables 3 and 4. Histology was performed according to manufacturer's instructions (Surgiopath). Edu was detected by Alexa Fluor 649 (Invitrogen).

Cell culture. Myoblasts were isolated and cultured on collagen-coated dishes (VWR) as described[23]. 4-OH tamoxifen (0.4 μM, Calbiochem) was added at the beginning of culture. For quantitative studies, cells were passed (1:3 dilution) every 4 days. For immunofluorescence, cells were plated onto 8-well chamber slides.

Muscle fibre size. Digital images of X-galactosidase and histologically stained sections were processed by Metamorph software (Molecular Devices). Parameters were chosen to define muscle fibre boundaries, which were re-examined visually for accuracy before quantification. Determination of fibre diameter and inner radius was assisted by Metamorph. Measurements for 300 fibres per animal were subjected to statistical analysis by Excel (Microsoft).

Full Methods and any associated references are available in the online version of the paper at www.nature.com/nature.

Received 15 April; accepted 16 June 2009.
Published online 25 June 2009.

1. Relaix, F., Rocancourt, D., Mansouri, A. & Buckingham, M. A. Pax3/Pax7-dependent population of skeletal muscle progenitor cells. *Nature* **435**, 948–953 (2005).
2. Seale, P. *et al.* Pax7 is required for the specification of myogenic satellite cells. *Cell* **102**, 777–786 (2000).
3. Oustanina, S., Hause, G. & Braun, T. Pax7 directs postnatal renewal and propagation of myogenic satellite cells but not their specification. *EMBO J.* **23**, 3430–3439 (2004).
4. Kuang, S., Charge, S. B., Seale, P., Huh, M. & Rudnicki, M. A. Distinct roles for Pax7 and Pax3 in adult regenerative myogenesis. *J. Cell Biol.* **172**, 103–113 (2006).

5. Relaix, F. *et al.* Pax3 and Pax7 have distinct and overlapping functions in adult muscle progenitor cells. *J. Cell Biol.* **172,** 91–102 (2006).
6. Zammit, P. S. *et al.* Pax7 and myogenic progression in skeletal muscle satellite cells. *J. Cell Sci.* **119,** 1824–1832 (2006).
7. Olguin, H. C., Yang, Z., Tapscott, S. J. & Olwin, B. B. Reciprocal inhibition between Pax7 and muscle regulatory factors modulates myogenic cell fate determination. *J. Cell Biol.* **177,** 769–779 (2007).
8. Seale, P., Ishibashi, J., Scime, A. & Rudnicki, M. A. Pax7 is necessary and sufficient for the myogenic specification of $CD45^{+}$:$Sca1^{+}$ stem cells from injured muscle. *PLoS Biol.* **2,** E130 (2004).
9. Guo, Q., Loomis, C. & Joyner, A. L. Fate map of mouse ventral limb ectoderm and the apical ectodermal ridge. *Dev. Biol.* **264,** 166–178 (2003).
10. Charge, S. B. & Rudnicki, M. A. Cellular and molecular regulation of muscle regeneration. *Physiol. Rev.* **84,** 209–238 (2004).
11. Schienda, J. *et al.* Somitic origin of limb muscle satellite and side population cells. *Proc. Natl Acad. Sci. USA* **103,** 945–950 (2006).
12. Kuang, S., Kuroda, K., Le Grand, F. & Rudnicki, M. A. Asymmetric self-renewal and commitment of satellite stem cells in muscle. *Cell* **129,** 999–1010 (2007).
13. Feil, R., Wagner, J., Metzger, D. & Chambon, P. Regulation of Cre recombinase activity by mutated estrogen receptor ligand-binding domains. *Biochem. Biophys. Res. Commun.* **237,** 752–757 (1997).
14. Soriano, P. Generalized lacZ expression with the ROSA26 Cre reporter strain. *Nature Genet.* **21,** 70–71 (1999).
15. Sacco, A., Doyonnas, R., Kraft, P., Vitorovic, S. & Blau, H. M. Self-renewal and expansion of single transplanted muscle stem cells. *Nature* **456,** 502–506 (2008).
16. Cerletti, M. *et al.* Highly efficient, functional engraftment of skeletal muscle stem cells in dystrophic muscles. *Cell* **134,** 37–47 (2008).
17. Bigard, A. X. *et al.* Changes in myosin heavy chain profile of mature regenerated muscle with endurance training in rat. *Acta Physiol. Scand.* **165,** 185–192 (1999).
18. Hayashi, S. & McMahon, A. P. Efficient recombination in diverse tissues by a tamoxifen-inducible form of Cre: a tool for temporally regulated gene activation/inactivation in the mouse. *Dev. Biol.* **244,** 305–318 (2002).
19. Koushik, S. V., Chen, H., Wang, J. & Conway, S. J. Generation of a conditional *loxP* allele of the *Pax3* transcription factor that enables selective deletion of the homeodomain. *Genesis* **32,** 114–117 (2002).
20. Pastoret, C. & Sebille, A. Age-related differences in regeneration of dystrophic (mdx) and normal muscle in the mouse. *Muscle Nerve* **18,** 1147–1154 (1995).
21. Brack, A. S. *et al.* Increased Wnt signaling during aging alters muscle stem cell fate and increases fibrosis. *Science* **317,** 807–810 (2007).
22. Hogan, B., Beddington, R., Costantini, F. & Lacey, E. *Manipulating the Mouse Embryo: A Laboratory Manual* 2nd edn (Cold Spring Harbor Laboratory Press, 1994).
23. Springer, M. L., Rando, T. A. & Blau, H. M. Gene delivery to muscle. *Curr. Protoc. Hum. Genet.* Unit 13.4 doi:10.1002/0471142905.hg1304s31 (2002).

Supplementary Information is linked to the online version of the paper at www.nature.com/nature.

Acknowledgements We thank E. Dikovskaia and E. Siple for technical assistance and Y. Zheng, A. Spradling, S.-J. Lee and J. J. Weyers for comments on the manuscript. D. Barry and K. R. Wagner taught us muscle injury techniques and sample preparation. The Carnegie Institution, NIH and Riley Children's Foundation provided funding for this work.

Author Contributions C.L. and C.-M.F. designed and conducted the research. S.J.C. provided the $Pax3^{f}$ allele and invaluable information. All three authors contributed to manuscript writing.

Author Information Reprints and permissions information is available at www.nature.com/reprints. Correspondence and requests for materials should be addressed to C.L. (lepper@ciwemb.edu) or C.-M.F. (fan@ciwemb.edu).

METHODS

Animals. The experimental outlines for making the *Pax7*^{f} and *Pax7*^{CE} alleles are in Supplementary Figs 1 and 2, respectively. The precise constructions for these alleles will be described elsewhere. The genetic crosses to remove the neo selection marker with actin-Flip mice are described (Supplementary Figs 1 and 2). Generation of the germline *Pax7*$^{\Delta}$ allele with Nestin-Cre mice is also outlined (Supplementary Fig. 1). Methods for genotyping and characterization of these alleles are described in the Supplementary figure legends.

To obtain *Pax7*$^{CE/f}$;*R26R*$^{+/-}$ and *Pax7*$^{+/CE}$;*R26R*$^{+/-}$ progenies for analysis, *Pax7*$^{+/CE}$ mice were mated to *Pax7*$^{+/f}$;*R26R*$^{+/-}$ animals. To obtain *Pax7*$^{CE/CE}$;*R26R*$^{+/-}$ animals, *Pax7*$^{+/CE}$;*R26R*$^{+/-}$ mice were mated to *Pax7*$^{+/CE}$ animals. Similar strategies of genetic crosses were used (excluding *R26R*$^{+}$) to obtain *cre/Esr1*$^{+/-}$;*Pax3*$^{f/f}$;*Pax7*$^{f/f}$ and *cre/Esr1*$^{+/-}$;*Pax7*$^{+/f}$ animals. Genotypes of these animals were determined by PCR using primers and conditions in Supplementary Table 1.

Tamoxifen. Tamoxifen (Sigma) was prepared by dissolving a freshly opened bottle of 5 g of tamoxifen in corn oil (Sigma) at 20 mg ml^{-1}. The mixture was incubated at 37 °C with periodic vortexing until tamoxifen was completely dissolved (~2–4 h). It was then divided into 10-ml conical tubes (VWR) and frozen in a −80 °C freezer. Each tube was thawed as needed and kept at 4 °C to be used for no more than 1 week. A 1-ml syringe with a 26-gauge needle was used for injection. Either intraperitoneal (for animals more than 3 weeks old) or subcutaneous (for animals less than 3 weeks old) delivery routes were used. The regimens are outlined in Figs 1a and 2i and Supplementary Fig. 8a.

Cardiotoxin. Cardiotoxin (Sigma) was prepared by dissolving a freshly opened tube in PBS at 10 μM. The solution was divided into Eppendorf tubes as 1-ml aliquot stocks, flash frozen, and stored at −80 °C. Each tube was thawed fresh before injection and not re-used. Animals were anaesthetized by intraperitoneal injection of Avertin (2,2,2-tribromoethanol from TCI America at 15 μl per gram body weight of 20 mg ml^{-1} solution). Right-leg tibialis anterior muscles were injected with 100 or 50 μl of cardiotoxin using an insulin needle (3/10cc Insulin Syringe from Becton Dickinson). For two rounds of injury, right-leg tibialis anterior muscles were initially injected with 100 μl of cardiotoxin and allowed to regenerate for 2 weeks. Following this, right-leg tibialis anterior muscles were re-injured via injection of 50 μl of cardiotoxin (see Fig. 2i). The volume and concentration of cardiotoxin are standard protocol used in published work[24–27]. Cardiotoxin animals were kept under a warming lamp until recovery before being returned to a normal cage rack.

EdU. For cultured cells, EdU supplied in the Click-iT EdU cell proliferation assay kit (Invitrogen) was used as instructed with minor modifications: EdU was used at 10 μM for 8 h in culture media; for detection, we performed immunostaining for primary and secondary antibodies (see below for a detailed protocol) first, then the click chemical reaction using Alexa Fluor 647 as a reactive fluorophore for detection, followed by DAPI staining (at 1 μg ml^{-1}).

For animals, EdU powder was dissolved in PBS at 0.5 mg ml^{-1} and frozen at −20 °C for long-term storage. EdU was injected at 0.1 mg per 20 g bodyweight intraperitoneally. The regimen for *in vivo* EdU injection for short-term proliferation and long-term retention assays are outlined in corresponding figures (Fig. 2i and Supplementary Fig. 8a, respectively). As for cultured cells, we performed the click chemical reaction using the same kit after immunostaining with primary and secondary antibodies and before DAPI staining (when applicable).

PCR genotyping and RT–PCR. For adult animals, tail DNA was used for genotyping by PCR. For newborns and animals younger than 21 days, toe DNA was used. DNA was extracted using the ExtractN'Amp kit (Sigma) following the manufacturer's instruction. One microlitre of neutralized DNA samples was used for PCR reaction using GoTaq polymerase (Promega) with buffers supplied by the manufacturer with 0.1 mM dNTPs and 2.5 mM $MgCl_2$. The PCR products were resolved in 2% agarose gel, stained with 0.5 μg ml^{-1} ethidium bromide (Gibco), and digitally imaged with a Bio-Rad Gel Doc system for record keeping.

Total RNA from injured tibialis anterior muscles was isolated using TRIzoL Reagent (Invitrogen) according to manufacturer's instructions. cDNA synthesis was performed using M-MLV Reverse Transcriptase (Invitrogen) also according to manufacturer's instructions. cDNA samples were then used for PCR as above.

Primer sequences, product sizes and PCR conditions used for genotyping and RT–PCR are in Supplementary Tables 1 and 2.

P0 animals to be used for satellite cell isolation were genotyped in the morning and killed in the afternoon according to their determined genotypes.

Western blot. Tibialis anterior muscles were harvested (time as indicated in each figure) and snap frozen in 1.5-ml Eppendorf tubes and stored at −80 °C until use. For protein extraction, frozen samples were weighed and suspended in 1:9 (weight to volume) of ice-cold RIPA buffer containing protease inhibitor cocktail (Roche) at 2× concentration and 1 mM PMSF, and ground with a sterile plastic mini-pestle (VWR) until no muscle bits were observable. The muscle homogenate was spun for 10 min in a microcentrifuge at maximum speed at 4 °C. 4× SDS sample buffer was added to the supernatant to reach 1× concentration. Samples were boiled for 5 min before being subjected to 7.5% SDS–PAGE. Kaleidoscope wide-range molecular mass marker (Bio-Rad) was used for size. Western transfer was performed with low molecular mass transfer buffer to an ECL membrane (Amersham) overnight at 30 V using a Bio-Rad mini-protein II transfer set up at 4 °C. Membrane was blocked in 5% low-fat carnation milk powder in TBS for 30 min, incubated with primary antibody in blocking solution overnight at 4 °C (mouse IgG1 anti-Pax7 at 1:50 and mouse IgG1 anti-α-tubulin (DM1α, from Sigma) at 1:10,000), washed in TBS, 3×, 10 min each, incubated with secondary antibody (HRP-conjugated anti-mouse IgG1 from Zymed at 1:3,000) in blocking solution for 1 h, washed in TBS, 3×, 10 min each, and then subjected to ECL reaction using the kit from Amersham (ECL Western Blotting Detection Reagents) and exposed to X-ray films. Standard solutions prepared for SDS–PAGE, western transfer, TBS and 4× sample buffer were as described previously[28].

X-galactosidase reaction and histology. Ten-micrometre frozen muscle sections (by Leica CM3000 Cryostat) were collected on Superfrost plus slides (VWR) and air dried for 30–90 min. Slides were either stored in a −20 °C freezer or used immediately.

For X-galactosidase reactions, sections were fixed with 0.2% glutaraldehyde/0.1 M phosphate buffer (pH 7.2) with 5 mM EGTA, 1 mM $MgCl_2$, for 5 min on ice, then washed and stained according to ref. 22 for 8–24 h to obtain satisfactory staining intensity. Stained sections were then washed in H_2O and stained with NFR (Lab Vision) for 5 min, rinsed with H_2O, dehydrated through graded EtOH series (25%, 50%, 75%, 95%, 100%), then in xylene and finally mounted in Permount mounting media (Fisher) with a coverslip (VWR).

For histology, sections were fixed in 4% paraformaldehyde/0.1 M phosphate (pH 7.2) for 30 min, rinsed with tap water, stained with Gill II haematoxylin for 5 min, washed with tap water, treated with Scott's tap water substitute for 10–15 s until staining colour turned blue, washed with tap water, stained with eosin for 1 min, destained in 95% EtOH, followed by 100% EtOH, xylene, then mounted in Permount with a coverslip. Staining reagents were purchased from Surgipath and used as instructed. Van Gieson stains were performed precisely as described[29].

Digital images of X-galactosidase stained and histological sections were taken using a SPOT camera and a Nikon Eclipse E800 vertical microscope.

Immunostaining. Freshly prepared 4% paraformaldehyde/0.1 M phosphate buffer (pH 7.2) was filtered through a 0.2-μm polyethersulphone filter (VWR) and chilled on ice. Paraformaldehyde solution was used within 12 h. Ten-micrometre frozen sections on Superfrost plus slides were fixed for exactly 12 min on ice, rinsed with 0.1 M phosphate buffer 3×, 5 min each, then permeabilized with 0.3% Triton X-100/PBS for 20 min. Sections were then incubated with mouse IgG blocking solution from the M.O.M. kit (Vector Lab) diluted in PBS/0.01% Triton X-100 following the dilution instructed in the manual. They were then incubated in blocking solution provided in the M.O.M. kit with an additional 15% goat serum in PBS/0.01% Triton X-100 for 20 min. Slides were then incubated with primary antibodies diluted (sources and dilution factors for each antibody are in Supplementary Table 3) in the blocking solution overnight at 4 °C. Next morning, the slides were washed 3× in PBS/0.01% Triton X-100 (all washes used this solution), 5 min each. Fluorescently conjugated secondary antibodies to each species-specific IgG in blocking solution was applied at dilutions in Supplementary Table 4 for 30 min. For Pax7 and M-Cad monoclonal IgG1 antibodies, the anti-IgG1 isotype-specific secondary antibody gave us the best result. The slides were washed again as after the primary antibody. If EdU was to be detected, we performed the click chemical reaction after this step according to manufacturer's instructions using the Click-iT kit components (Invitrogen). The slides were then washed, incubated with DAPI when applicable (at 1 μg ml^{-1}) for 10 min, washed two more times, and mounted in FluoromountG solution (Southern Biotechnology) with a coverslip. All images were taken under an Axioscope equipped with AxioCam with filters of non-overlapping spectra (according to the fluorophores used) for multiple fluorescent signals. Images were pseudo-coloured and superimposed (when necessary) using the MetaMorph program.

For cultured cells, 8-well chamber slides were fixed and processed the same way as sections except that the mouse IgG blocking (M.O.M. kit) step was omitted.

Myoblast cell culture. Genotyped animals were killed by cervical dislocation, and hindlimb muscles were removed and minced by razor blades. Each sample was digested with collagenase and dispase as described in ref. 23. Dissociated muscles were then transferred to 15 ml conical tubes with 10 ml myoblast media without FGF, spun down in the clinical centrifuge and re-suspended in culture media with 2.5 ng ml^{-1} bFGF.

For cell counting and marker analysis, 0.4 μM 4-OH tamoxifen (Calbiochem) was applied at the same time of cell plating. Each sample was divided into three parts. One part was plated on a 3-cm collagen-coated dish (prepared as described in ref. 23) for cell counting 4 days later. One part was plated on another 3-cm collagen-coated dish but used for sequential passaging at 1:3 dilution. The remaining part was plated into 8-well chamber slides (coated with collagen) for immunostaining. For passaging, cells were passaged at 1:3 dilution every 4 days. At each round, each sample was divided into three parts; the same routine as above for cell counting, continuous passaging and immunostaining was repeated. For quantification of β-gal$^+$ cell numbers, the 3-cm dish was fixed and subjected to X-galactosidase staining (see above), and nine random fields were imaged using the Canon EOS30D camera attached to the Zeiss SV11 APO microscope at the highest magnification (each frame is of 1.33 mm^2 area, 0.95 mm × 1.4 mm), and β-gal$^+$ cells (blue) counted and scored for their morphology. Cells that displayed large flattened multi-cellular processes were scored as 'fibroblastic'. For immunostaining quantification, 9–16 random fields per well were chosen for imaging and quantified for EdU labelling or marker expression in conjunction with anti-β-gal antibody staining.

For myogenic marker analysis, myoblast cultures were first treated with or without 4-OH tamoxifen for 2 days for gene inactivation. They were then assayed for myoblast markers (Pax3, Pax7, desmin or MyoD) by RT–PCR or immunostaining, or incubated with Edu (10 μM for 8 h) for proliferation assays. For differentiation, cells were switched to differentiation media (5% horse serum in DME; ref. 23) for 3–4 days and assayed for myogenin and MHC expression.

Muscle fibre quantification. Cross-sections (by cryostat sections at 10 μm) of tibialis anterior muscles were stained by X-galalactosidase reactions or by haematoxylin and eosin. Digital images were acquired with a CCD camera by routine brightfield microscopy. Image processing and morphometry were carried out using MetaMorph software (Molecular Devices). Specifically, myofibres were automatically delineated. Myofibre outlines were visually examined to assure accuracy before further analysis. The centroid (geometric centre) of each myofibre was then determined to calculate the myofibre inner radius, the distance from the centroid to the closest edge. A circle of this radius will be completely contained (inscribed) within the myofibre outline. Therefore, this is the most conservative measure of fibre size.

For myofibre diameter measurements, we used the 'largest diameter of the lesser aspect of the myofibre' criterion[30]. This measurement is conventionally used to assess fibre size. Automatic measurement of this dimension for outlined myofibres was also implemented in MetaMorph (termed 'Breadth' within the software).

Statistical analysis. Quantitative data displayed as histograms are expressed as means ± standard error of the mean (represented as error bars). Quantification of total percentages is shown in tables. Regenerated muscle fibre numbers are displayed as a distribution plot. ANOVA was conducted using an Excel spreadsheet by using a *t*-test for two-tailed paired comparison. Statistical significance was set at a P value <0.05.

24. Hu, P., Geles, K. G., Paik, J.-H., DePinho, R. A. & Tijan, R. Codependent activators direct myoblast-specific MyoD transcription. *Dev. Cell* **15,** 534–546 (2008).
25. Melcon, G. *et al.* Loss of emerin at the nuclear envelope disrupts the Rb1/E2F and MyoD pathways during muscle regeneration. *Hum. Mol. Genet.* **15,** 637–651 (2006).
26. Iezzi, S. *et al.* Deacetylase inhibitors increase muscle cell size by promoting myoblast recruitment and fusion through induction of follistatin. *Dev. Cell* **6,** 673–684 (2004).
27. Meeson, A. P. *et al.* Cellular and molecular regulation of skeletal muscle side population cells. *Stem Cells* **22,** 1305–1320 (2004).
28. Harlow, E. & Lane, D. *Antibodies: A Laboratory Manual* (Cold Spring Harbor Laboratory Press, 1988).
29. Bancroft, J. D. & Cook, H. D. *Manual of Histological Techniques and their Diagnostic Application* (Churchill Livingstone, 1994).
30. Dubowitz, V. *Muscle Biopsy: A Practical Approach* (Bailliere Tindall, 1985).